We are IntechOpen, the world's leading publisher of Open Access books Built by scientists, for scientists

6,900
Open access books available

186,000
International authors and editors

200M
Downloads

Our authors are among the

154
Countries delivered to

TOP 1%
most cited scientists

12.2%
Contributors from top 500 universities

WEB OF SCIENCE™

Selection of our books indexed in the Book Citation Index in Web of Science™ Core Collection (BKCI)

Interested in publishing with us?
Contact book.department@intechopen.com

Numbers displayed above are based on latest data collected.
For more information visit www.intechopen.com

20

Intelligent Vibration Signal Diagnostic System Using Artificial Neural Network

Chang-Ching Lin
Tamkang University Tamshui, Taipei County, Taiwan

1. Introduction

In today's sophisticated manufacturing industry maintenance personnel are constantly forced to make important, and often costly, decisions on the use of machinery. Usually, these decisions are based on practical considerations, previous experiences, historical data and common sense. However, the exact determination of machine conditions and accurate prognosis of incipient failures or machine degradation are key elements in maximizing machine availability.

The practice of maintenance includes machine condition monitoring, fault diagnostics, reliability analysis, and maintenance planning. Traditionally, equipment reliability studies depend heavily on statistical analysis of data from experimental life-tests or historical failure data. Tedious data collection procedures usually make this off-line approach unrealistic and inefficient for a fast-changing manufacturing environment (Singh & Kazzaz, 2003). Over the past few decades technologies in machine condition monitoring and fault diagnostics have matured. Many state-of-the-art machine condition monitoring and diagnostic technologies allow monitoring and fault detection to perform in on-line, real-time fashion making maintenance tasks more efficient and effective. Needless to say, new technologies often produce new kinds of information that may not have been directly associated with the traditional maintenance methodologies. Therefore, how to integrate this new information into maintenance planning to take advantages of the new technologies has become a big challenge for the research community.

From the viewpoint of maintenance planning, Condition Based Maintenance (CBM) is an approach that uses the most cost effective methodology for the performance of machinery maintenance. The idea is to ensure maximum operational life and minimum downtime of machinery within predefined cost, safety and availability constraints. When machinery life extension is a major consideration the CBM approach usually involves predictive maintenance. In the term of predictive maintenance, a two-level approach should be addressed: 1) need to develop a condition monitoring for machine fault detection and 2) need to develop a diagnostic system for possible machine maintenance suggestion.

The subject of CBM is charged with developing new technologies to diagnose the machinery problems. Different methods of fault identification have been developed and used effectively to detect the machine faults at an early stage using different machine quantities, such as current, voltage, speed, efficiency, temperature and vibrations. One of the principal tools for diagnosing rotating machinery problems is the vibration analysis. Through the use

of different signal processing techniques, it is possible to obtain vital diagnostic information from vibration profile before the equipment catastrophically fails. A problem with diagnostic techniques is that they require constant human interpretation of the results. The logical progression of the condition monitoring technologies is the automation of the diagnostic process. The research has been underway for a long time to automate the diagnostic process. Recently, artificial intelligent tools, such as expert systems, neural network and fuzzy logic, have been widely used with the monitoring system to support the detection and diagnostic tasks.

In this chapter, artificial neural network (ANN) technologies and analytical models have been investigated and incorporated to present an Intelligent Diagnostic System (IDS), which could increase the effectiveness and efficiency of traditional condition monitoring diagnostic systems.

Several advanced vibration trending methods have been studied and used to quantify machine operating conditions. The different aspects of vibration signal and its processing techniques, including autoregressive (AR) parametric modeling and different vibration trending methods are illustrated. An example of integrated IDS based on real-time, multi-channel and neural network technologies is introduced. It involves intermittent or continuous collection of vibration data related to the operating condition of critical machine components, predicting its fault from a vibration symptom, and identifying the cause of the fault. The IDS contains two major parts: the condition monitoring system (CMS) and the diagnostic system (DS). A neural network architecture based on Adaptive Resonance Theory (ART) is introduced. The fault diagnostic system is incorporated with ARTMAP neural network, which is an enhanced model of the ART neural network. In this chapter, its performance testing on simulated vibration signals is presented. An in-depth testing using lab bearing fault signals has been implemented to validate the performance of the IDS. The objective is to provide a new and practicable solution for CBM.

Essentially, this chapter presents an innovative method to synthesize low level information, such as vibration signals, with high level information, like signal patterns, to form a rigorous theoretical base for condition-based predictive maintenance.

2. Condition monitoring system

The condition monitoring system developed contains four modules (see Fig. 1): data acquisition, Parameters Estimation (PE), Performance Monitoring (PM), and Information Display and Control (IDC). The entire system was coded using C programming language. We have developed a user friendly graphic interface that allows for easy access and control in monitoring an operating machine. The system has been tested and verified on an experimental lab setting. The detailed procedure of ISDS and programming logic is discussed in the following sections.

2.1 Data acquisition module

The data acquisition module is more hardware related than the other modules. Vibration signals were acquired through accelerometers connected to a DASMUX-64 multiplexer board and a HSDAS-16 data acquisition board installed in a PC compatible computer. The multi-channel data acquisition program controlling the hardware equipment has been coded.

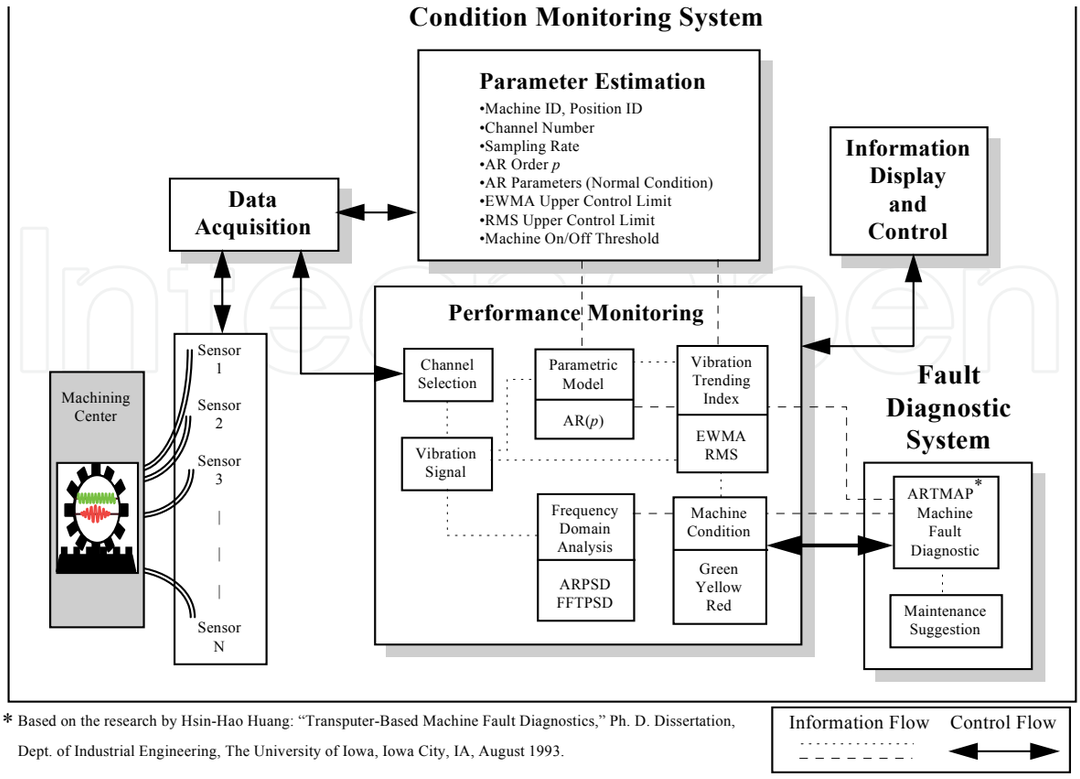

Fig. 1. Overview of intelligent diagnostic system

2.2 Programming logic for Parameter Estimation (PE) module

The parameter estimation module is designed to estimate the parameters of the normal condition of a machine. It provides a procedure to set up the machine positions considered to be critical locations of the machine. The PE module must be executed before running the PM module. The information to be calculated in the PM module needs to be compared to the base-line information generated in the PE module.

The normal operating condition of a machine position is usually defined by experience or from empirical data. Generally speaking, a particular operation mode of a machine is selected and then defined as a "normal condition". However, this normal condition is not unchangeable. Any adjustment to the machine, such as overhaul or other minor repairs, would change its internal mechanisms. In this case, the normal condition must be redefined, and all the base-line data of the monitored positions on the machine need to be reset.

The PE procedure starts with specifying the ID of a machine, its location ID, and several other parameters related to each position, such as channel number and sampling rate. Then the upper control limits of the Exponentially Weighted Moving Average (EWMA) (Spoerre, 1993) and Root Mean Square (RMS) (Monk, 1972; Wheeler 1968) vibration trending indices are determined and an adequate Autoregressive (AR) order is computed. The AR time series modelling method is the most popular parametric spectral estimation method which translates a time signal into both frequency domain and parameter domain (Gersch, 1976). Once the AR order is determined, the AR parameters can be estimated through several normal condition signals collected from the particular position. A major issue with the parametric method is determining the AR order for a given signal. It is usually a trade-off between resolution and unnecessary peaks. Many criteria have been proposed as objective functions for selecting a

"good" AR model order. Akaike has developed two criteria, the Final Prediction Error (FPE) (Akaike, 1969) and Akaike Information Criterion (AIC) (Akaike, 1974). The criteria presented here may be simply used as guidelines for initial order selection, which are known to work well for true AR signals; but may not work well with real data, depending on how well such data set is modelled by an AR model. Therefore, both FPE and AIC have been adapted in this research for the AR order suggestion.

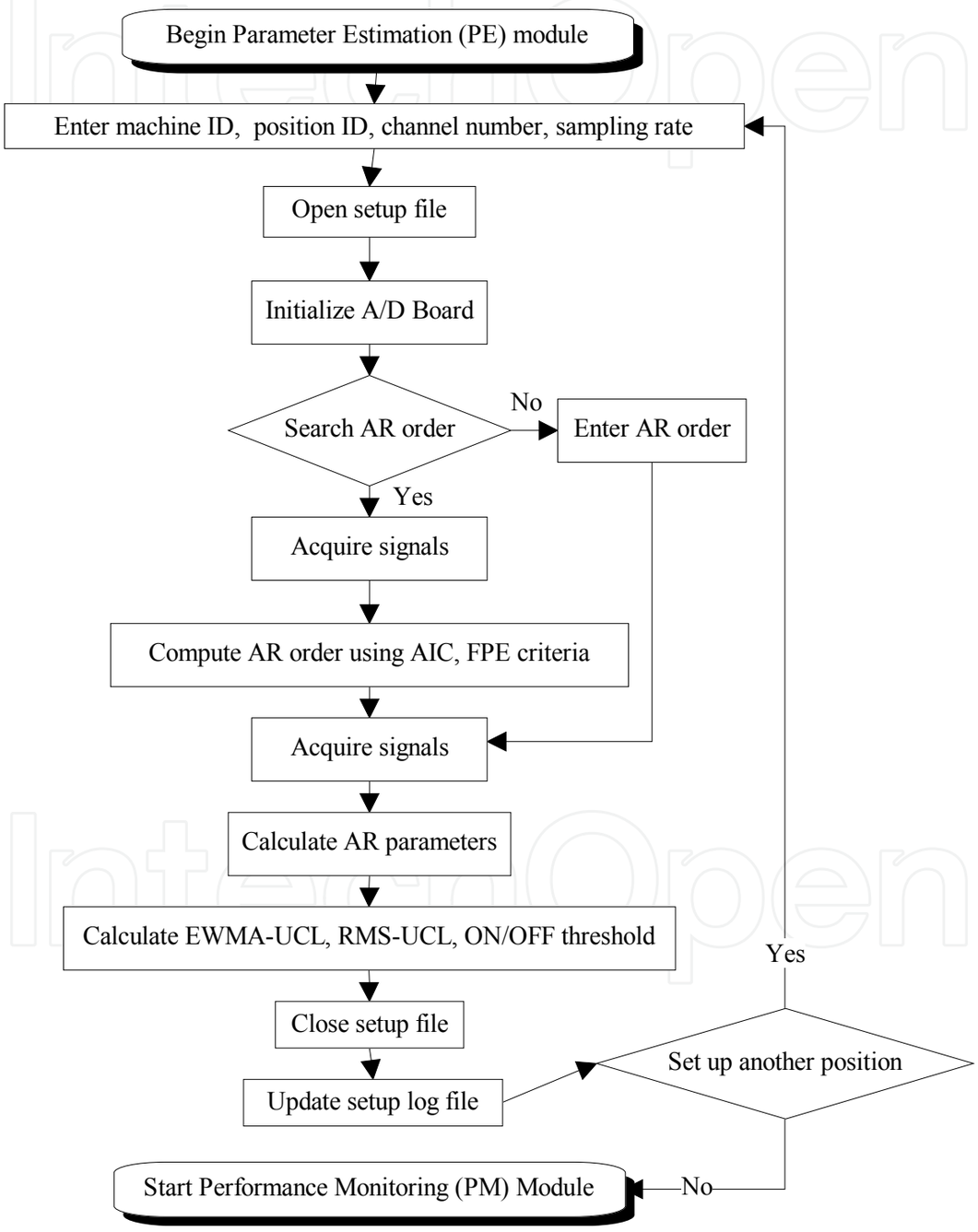

Fig. 2. Flowchart of parameter estimation (PE) module

A setup file is then generated after the PE procedure is completed. This file, given a name that combines the machine ID and the position ID, consists of all the parameters associated with the specific position. The number of setup files created depends on the number of positions to be monitored in the PM mode, that is, each monitored position is accompanied by a setup file.
In order to perform a multi-channel monitoring scheme a setup log file is also generated. This file contains all the names of setup files created in the PE mode. Every time a new position is added its setup file name is appended to the setup log file. The setup log file is very important. It not only determines the channels needing to be scanned when the PM program is executed, it also provides the PM program with paths to locate all the necessary information contained in the setup files. Fig. 2 shows the programming logic of the PE module. In practice, after the PE procedure is completed, on-line performance monitoring of the machine (the PM mode) begins.

2.3 Programming logic for Performance Monitoring (PM) module

In the PM module, vibration data arrive through the data acquisition hardware and are processed by AR, EWMA, ARPSD, RMS, FFT spectrum, and hourly usage calculation subroutines. After each calculation the current result is displayed on the computer screen through the Information Display and Control (IDC) module. Fig. 3 illustrates the flow chart of the PM programming logic.
IDC is in charge of functions such as current information displaying, monitoring control, and machine status reasoning. Details of these functions are given in the following section.

2.4 Information Display and Control (IDC) module

Eight separate, small windows appear on the computer screen when the IDC module is activated. Each window is designed to show the current reading and information related to each calculation subroutine (e.g. AR, EWMA, ARPSD, RMS, and FFT spectrum) for the current position being monitored.
Window 1 is designed to plot the current time domain data collected from the data acquisition equipment. Window 2 displays both the AR parameter pattern of the current signal and the normal condition AR parameter pattern stored in the setup file generated in the PE module. Window 3 plots the current EWMA reading on a EWMA control chart and its upper control limit. Window 4 plots the current RMS value and its upper control limit on a RMS control chart. Both the RMS and EWMA upper control limits are calculated in the PE module. Window 5 displays the hourly usage and other information of the position. The hourly usage of the position is calculated based on the vibration level of that position. It is an estimated running time of the component up to the calculating point from the time this position is set up. Window 6 indicates the current performance status of the position. Three different levels of performance status: normal, abnormal, and stop, are designed. Each status is represented by a different colour: a green light signals a normal condition; a yellow light represents an abnormal condition; and a red light indicates an emergency stop situation. The determination of the status of a position based on the current readings is discussed in the next section. Window 7 gives the current ARPSD spectrum, which is calculated based on the AR parameters from Window 2. Finally, Window 8 displays the current FFT spectrum by using the time domain data from Window 1.
In addition to real-time information display, the IDC module also provides a user-friendly graphic interface for monitoring control. A user can utilize the mouse to navigate around

the computer screen and click on an icon to perform the specified function. For instance, to switch to another channel one can click on the "CH+" or "CH-" icon. Fig. 4 shows the IDC screen layout developed.

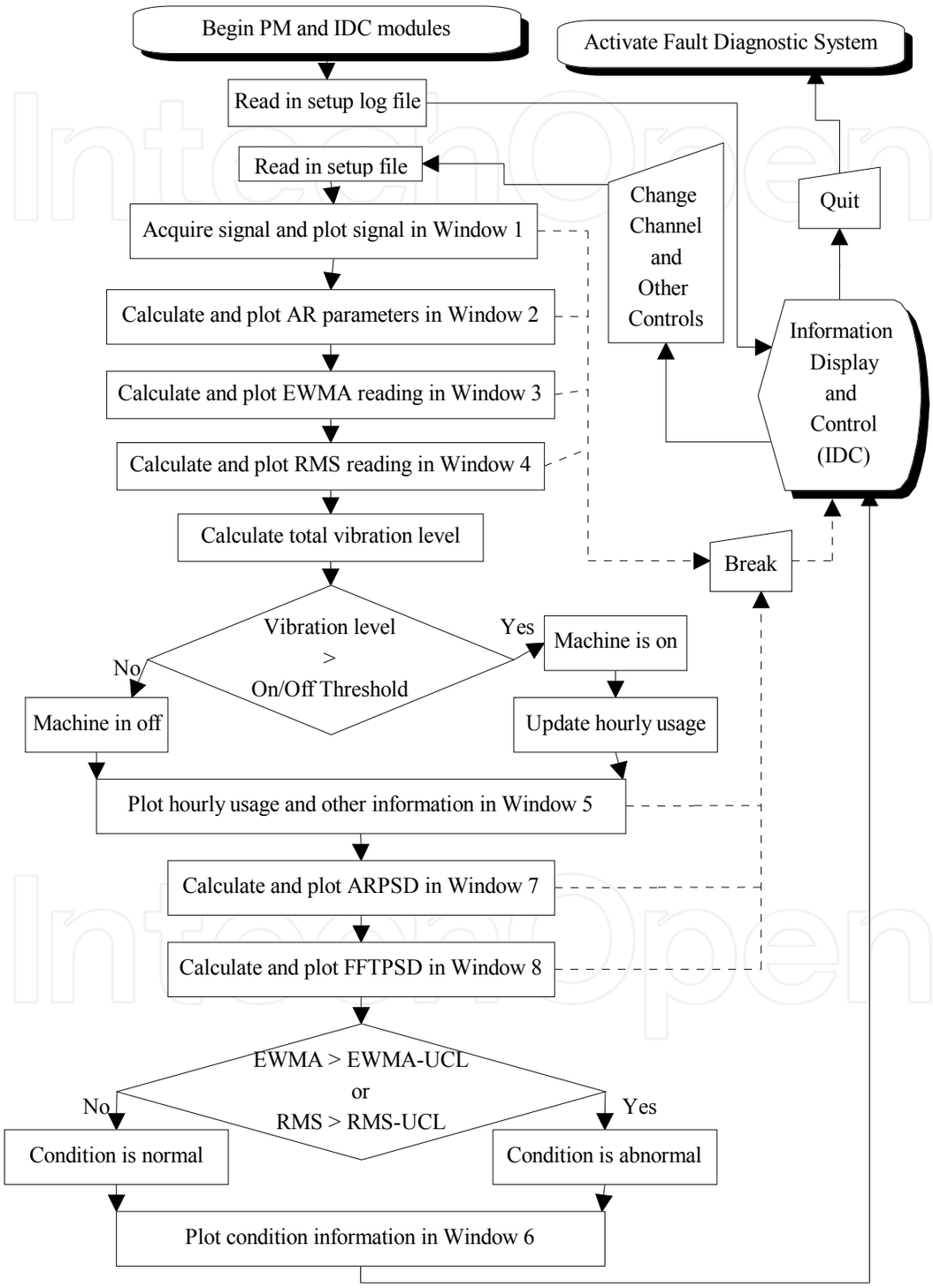

Fig. 3. Flowchart of PM and IDC modules

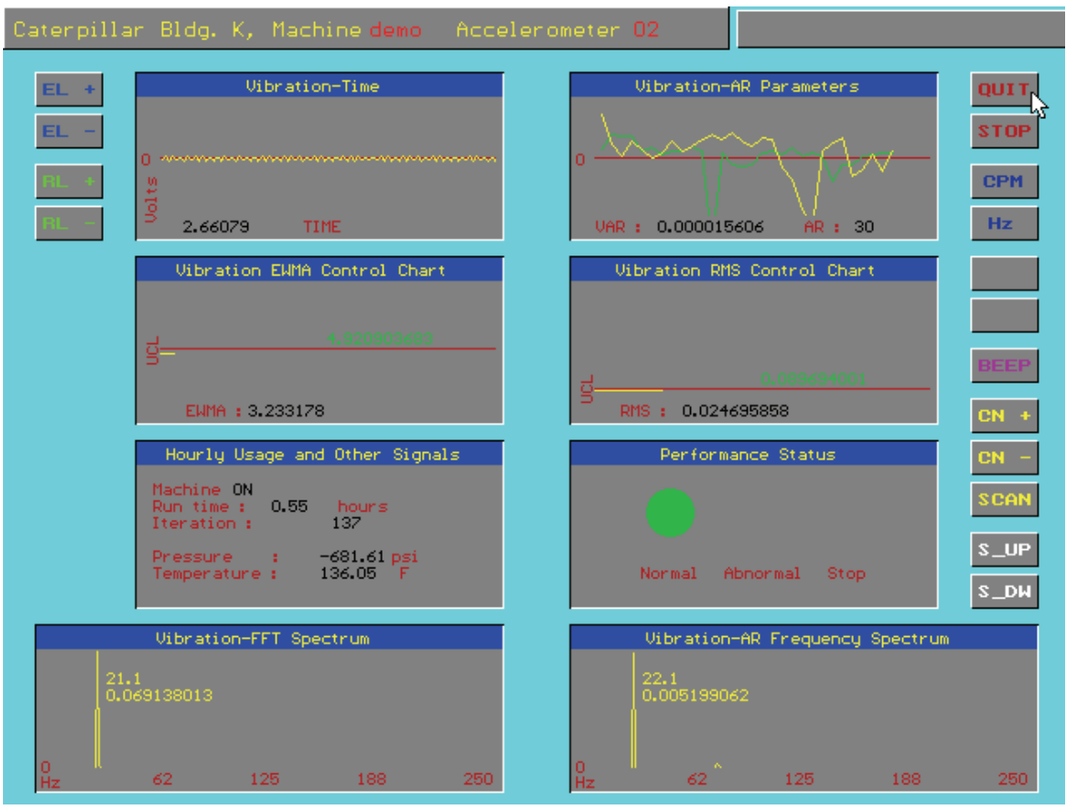

Fig. 4. Condition monitoring information display and control (IDC) Screen layout

2.5 Vibration condition status reasoning

Based on the criteria stored in the setup file and the current readings, the EWMA and RMS control charts show whether the current readings are under or above their respective upper control limit. If both readings are under their corresponding control limits, then the position is in a normal condition. However, if either one of the control readings exceeds its upper control limit, the performance status reasoning program would turn on the yellow light to indicate the abnormality of the position. In this case, the fault diagnostic system is activated.

2.6 Condition monitoring sample session

Data collection, in the form of vibration signals, was conducted using the following test rig (see Fig. 5): a 1/2 hp DC motor connected to a shaft by a drive belt, two sleeve bearings mounted on each end of the shaft and secured to a steel plate, an amplifier to magnify signals, a DASMUX-64 multiplexer board, and a HSDAS-16 data acquisition board installed in a personal computer. Vibration signals were collected from the bearing using 328C04 PCB accelerometers mounted on the bearing housings. Using the test rig, the following sample session was conducted.

Assume that when the motor was turned on initially, it was running in normal condition. Later, a small piece of clay was attached to the rotational element of the test rig to generate an imbalance condition. This was used as an abnormal condition in the experiment. In the beginning, the setup procedure (PE) needed to be performed in order to obtain the base-li information. The sampling rate used was 1000 Hz and the sampling time was one second.

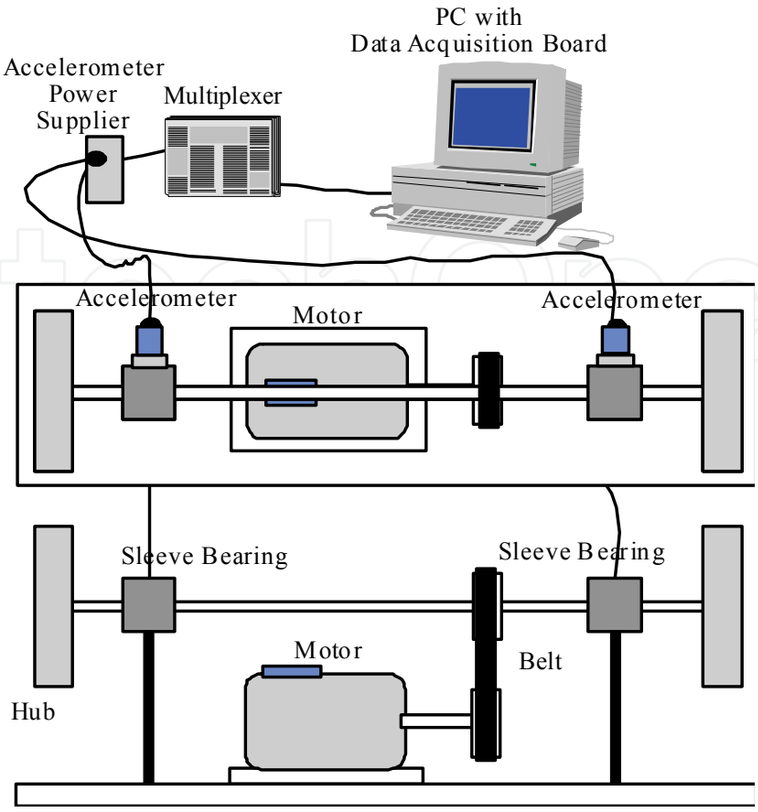

Fig. 5. The test rig for ISDS experiment

The PE program first acquired eight samples and then took their average. Using the average normal signal, the AIC and FPE criteria were calculated. An AR order suggestion for the normal condition of the test rig was made. The AR order was fixed throughout the entire experiment. Once the AR order was known, the program started estimating the AR parameters and upper control limits of RMS and EWMA by collecting another eight data sets, calculating eight sets of AR parameters, and then averaging them. Finally, all parameters were stored in the setup file which would be used in the PM stage. An example of the normal condition parameters from a setup file are listed below:

- Machine ID: TESTRG
- Position ID: CHN1
- Channel number: 1
- Sampling rate: 1000
- AR order: 32
- AR parameters: ....
- EWMAUCL: 0.8912
- RMSUCL: 0.0367

When the machine was running in normal condition the readings of EWMA were approximately -0.486 far below the EWMAUCL of 0.8912. The readings of RMS were about 0.01895, and therefore, they were below the RMSUCL. As soon as an imbalance condition was generated the EWMA and RMS readings jumped to values of 3.3259 and 0.0504, respectively. The EWMA and RMS readings indicated the test rig was in an abnormal condition since both readings exceeded their respective control limits.

The machine condition monitoring mode switches to diagnostic mode when at least one index exceeds its control limit. Once the system is in the diagnostic system, a detailed automatic analysis begins to identify the machine abnormality occurred. The next section explains the fault diagnostic system designed for this research.

3. ARTMAP-based diagnostic system

3.1 Introduction to ARTMAP neural network

The diagnostic system in this paper employs a neural network architecture, called Adaptive Resonance Theory with Map Field (ARTMAP). The fault diagnostic system is based on the ARTMAP fault diagnostic network developed by Knapp and Wang (Knapp & Wang, 1992). The ARTMAP network is an enhanced model of the ART2 neural network (Carpenter, 1987; Carpenter, 1991). The ARTMAP learning system is built from a pair of ART modules (see Fig. 6), which is capable of self-organizing stable recognition categories in response to arbitrary sequences of input patterns. These ART modules (ART_a and ART_b) are linked by Map Field and an internal controller that controls the learning of an associative map from the ART_a recognition categories to the ART_b recognition categories, as well as the matching of the ART_a vigilance parameter (ρ'). This vigilance test differs from the vigilance test inside the ART2 network. It determines the closeness between the recognition categories of ART_a and ART_b (Knapp, 1992).

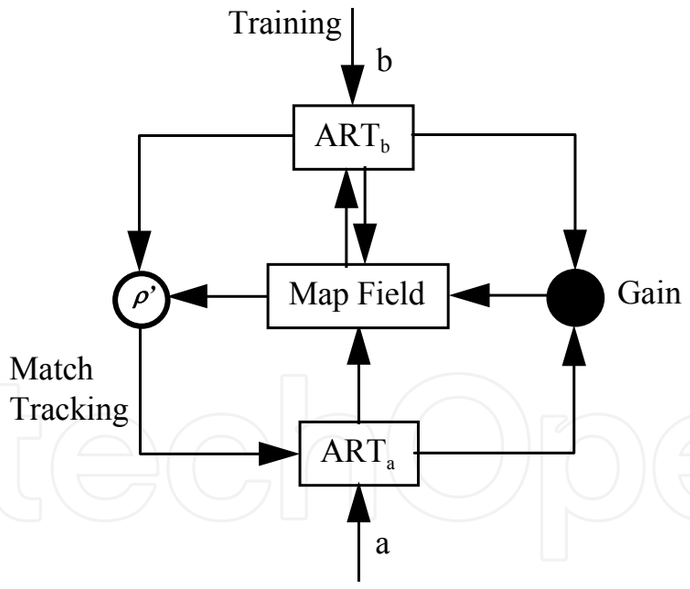

Fig. 6. ARTMAP architecture

A modified ARTMAP architecture has been adopted in this paper in order to perform the supervised learning. The modified ARTMAP architecture is based on the research by Knapp and Huang, which replaces the second ART module (ART_b) by a target output pattern provided by the user (Huang, 1993; Knapp, 1992). The major difference between the modified ARTMAP network and the ART2 network is the modified ARTMAP permits supervised learning while ART2 is an unsupervised neural network classifier. Fig. 7 shows the modified ARTMAP architecture.

3.2 Performance analysis of ARTMAP-based diagnostic system

The performance of the ARTMAP-based diagnostic system was validated by employing vibration signals from test bearings. A small adjustment was made on the experimental test rig shown in Figure 5. The two sleeve bearings were replaced by two ball bearings with steel housings. The new setup allows easy detachment of the ball bearing from the housing for exchanging different bearings. Figure 8 shows the modified experimental setup.

Six bearings with different defect conditions were made. Table 1 describes these defective ball bearings. A two-stage vibration data collection was conducted for each bearing. Five sets of vibration signals were collected in the first batch, three sets in the second batch. A total of eight sets of vibration signals were collected under each defect. Therefore, there were a total of 48 data sets. All time domain vibration signals were transformed and parameterized through the ARPSD algorithm. The AR order used was 30. Thus, the dimension number for each AR parameter pattern was 31 (i.e., 30 AR parameters plus one variance). These 48 AR parameter patterns were used to train and test the ARTMAP-based diagnostic system.

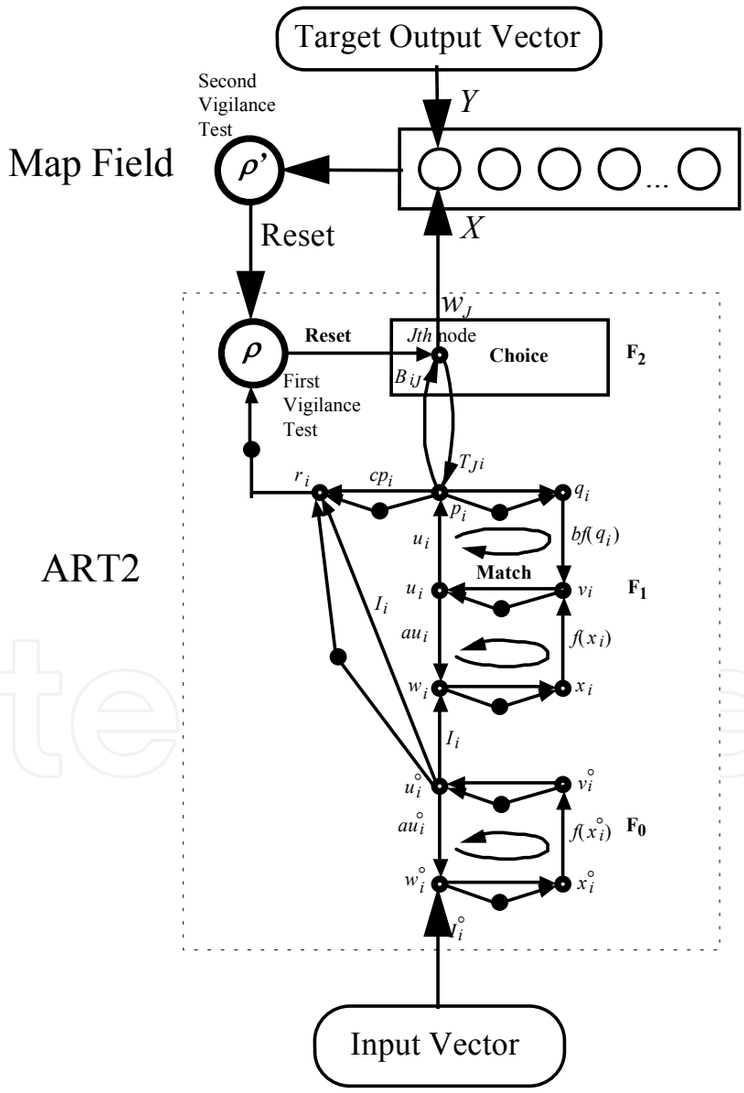

Fig. 7. Modified ARTMAP architecture

Bearing #	Defect
1	Good bearing
2	White sand in bearing
3	Over-greased in raceway
4	One scratch in inner race
5	One scratch in one ball
6	No grease in raceway

Table 1. Test ball bearings

Pattern Number		Bearing Number											
		1		2		3		4		5		6	
Batch 1	1	Train		Train		Train		Train		Train		Train	
	2	1	3	2	6	3	1	4	2	5	6	6	2
	3	1	6	2	6	3	1	4	2	5	4	6	1
	4	1	6	2	6	3	1	4	2	5	4	6	2
	5	1	6	2	6	3	1	4	2	5	6	6	1
Batch 2	1	1	3	2	6	3	1	**5**	**4**	5	4	6	5
	2	1	3	2	6	3	1	**5**	**4**	5	4	6	5
	3	1	3	2	6	3	1	**5**	**4**	5	4	6	5

Table 2. Bearing test results of ARTMAP-based ISDS

Note that the 512 frequency components in each ARPSD spectrum were compressed to only 31 parameters in each AR model indicating the system dealt with a significantly reduced amount of data; this is extremely beneficial in real-time applications.

Fig. 8 shows the plots of AR parameter patterns from the six defective bearings. The first column displays the six training patterns, which is the first one of the eight data sets from each bearing type. The second column illustrates some of the other seven test patterns, where the solid lines represent data from the first collection batch and the dotted lines are from the second batch. As can be seen from Fig. 8, the profiles of the AR parameter patterns within each group are very similar. Only a few deviations can be seen between the first and second batches. The deviations come from the very sensitive but inevitable internal structure changes of the setup during the bearing attachment and detachment operations between the two data collections.

The experimental procedure began with using the first pattern of all the conditions for training and then randomly testing the other seven patterns. In addition, the modified ARTMAP network was designed to provide two suggested fault patterns (i.e., the outputs of the first two activated nodes from the F_2 field). Table 2 summarizes the test results on diagnosing the 42 test patterns. The first column of Table 2 for each bearing type is the first identified fault from the network. It shows only 3 of the 42 test cases were mismatched in the first guess but they were then picked up correctly by the network in the second guess (see bold-face numbers in Table 2). Interestingly, these three mismatched patterns were from

the second batch. If the profiles of Bearings 4 and 5 in the second batch (the dotted profiles in the second column of Fig. 8) were compared, then one could see the test patterns of Bearing 4 from the second batch were much closer to the training pattern of Bearing 5 than that of Bearing 4. This is why the network recognized the test patterns of Bearing 4 as Bearing 5 in its first guess. These test results clearly display the capability and reliability of the ARTMAP-based diagnostic system and the robustness of using AR parameter patterns to represent vibration signals. For the efficiency of the ARTMAP training, the training time of one 31-point AR parameter pattern was less than one second on a PC.

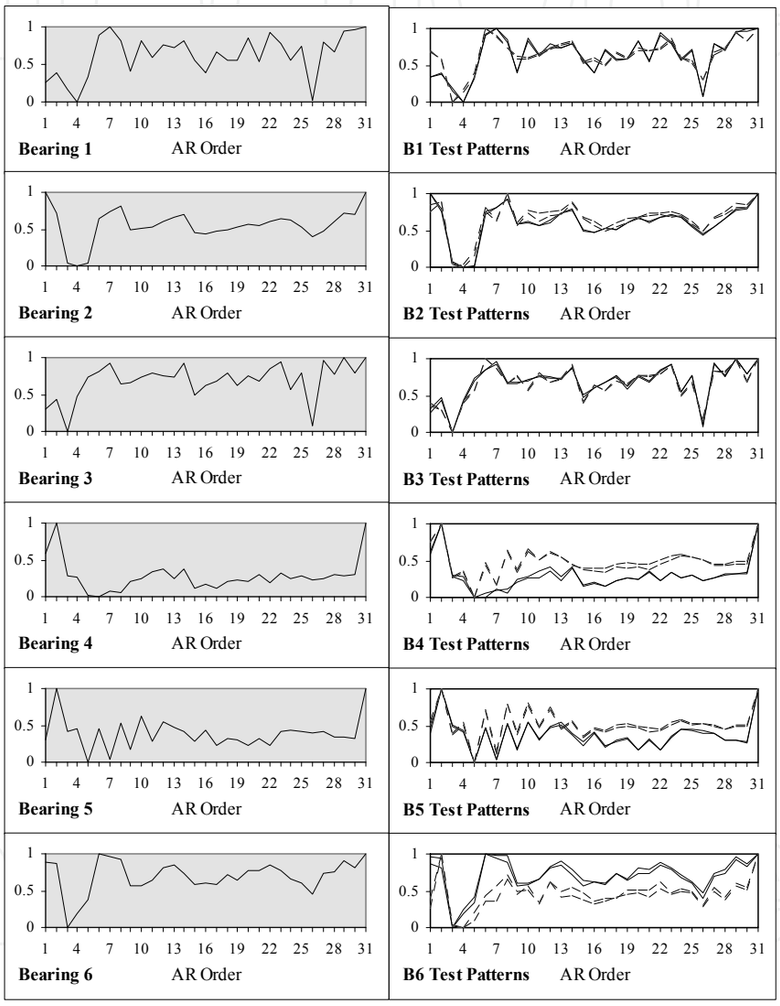

Fig. 8. AR parameters patterns of defective bearings

4. Summary and conclusions

This paper presents an integrated Intelligent Diagnostic System (IDS). Several unique features have been added to ISDS, including the advanced vibration trending techniques, the data reduction and features extraction through AR parametric model, the multi-channel and on-line capabilities, the user-friendly graphical display and control interface, and a unique machine diagnostic scheme through the modified ARTMAP neural network.

Based on the ART2 architecture, a modified ARTMAP network is introduced. The modified ARTMAP network is capable of supervised learning. In order to test the performance and robustness of the modified ARTMAP network in ISDS, an extensive bearing fault experiment has been conducted. The experimental results show ISDS is able to detect and identify several machine faults correctly (e.g., ball bearing defects in our case).

5. Appendix

5.1 Time series autoregressive (AR) parametric model

According to the features representation requirements in signal pattern recognition, if the features shown by raw data are ambiguous, then it is necessary to use a preprocessor or transformation method on the raw data. Such a preprocessor should have feature extraction capability that can invariably transfer raw data from one domain to another. The objective of this preprocessing stage is to reveal the characteristics of a pattern such that the pattern can be more easily identified.

The most important feature provided in vibration signals is frequency. Therefore, the characteristics of vibration signals can be shown clearly in the frequency domain. Traditionally, the Fast Fourier Transform (FFT) based spectral estimators are used to estimate the power spectral density (PSD) of signals. Recently, many parameter estimation methods have been developed. Among them, the autoregressive (AR) modeling method is the most popular (Gersch & Liu, 1976). The major advantage of using the parametric spectral estimation method is its ability to translate a time signal into both frequency (PSD) domain and parameter domain. In addition, parametric spectrum estimation is based on a more realistic assumption and does not need a long data record to get a high resolution spectrum.

5.2 Parametric autoregressive spectral estimation

Vibration signals can be treated as if they were generated from a time series random process. Now consider a time series x_n,

$$x_n, \quad n = -\infty, \ldots, 0, \ldots, \infty \tag{A.1}$$

where the observed interval is from n = 1, ..., N. The autoregressive model of x_n is given in Equation (A.2).

$$x_n = -a_1 x_{n-1} - a_2 x_{n-2} - \ldots - a_p x_{n-p} + e_n \tag{A.2}$$

where e_n is the prediction error, and p is the order of the model. The parametric spectrum may be computed by plugging all p a_k parameters into the theoretical power spectral density (PSD) function defined from Equation (A.3).

$$P_{AR}(f) = \frac{2\,\Delta t\ \sigma^2}{\left(1 + \sum_{k=1}^{P} a_k\ \exp\left(-i 2\pi f k \Delta t\right)\right)^2}$$
$$-\frac{1}{2} \le f \le \frac{1}{2} \tag{A.3}$$
$$\Delta t = \frac{1}{S}$$

where S is the sampling rate used in data acquisition, f is the fraction of the sampling rate, p is the prediction lag or order of the AR model, and σ^2 is the variance. Therefore, if the prediction coefficients, a_k, can be estimated accurately, the parametric spectrum, $P_{AR}(f)$, of the random process can be calculated correctly through Equation (A.3).

Several approaches are available for estimating the AR model parameters. It has been observed that if the data consist of sinusoids with white noise, the peak location in the AR spectral estimate critically depends on the phase of the sinusoid (Swingler, 1980). The degree of phase dependence varies with different parameter estimation methods. Of all the AR parameter estimation methods, the modified covariance method appears to yield the best results (Kay, 1988). The modified covariance method appears to yield statistically stable spectral estimates with high resolution (Kay, 1988). For data consisting of sinusoids with white noise, a number of desirable properties have been observed (Kay, 1988; Marple, 1987):

1. The shifting of the peaks from the true frequency locations due to additive noise appears to be less than many other AR spectral estimators.
2. The peak location affected by initial sinusoidal phase is considerably reduced.
3. Spectral line splitting in which a single sinusoidal component gives rise to two distinct spectral peaks has never been observed.

5.3 AR order selection

A major issue with the parametric method is determining the AR order for a given signal. It is usually a trade-off between resolution and unnecessary peaks. Many criteria have been proposed as objective functions for selecting a "good" AR model order. Akaike has developed two criteria, the final prediction error (FPE) (Akaike, 1969) and Akaike information criterion (AIC) (Akaike, 1974). The FPE for an AR process is defined as follows:

$$\mathrm{FPE}(p) = \hat{\sigma}_p{}^2 \left(\frac{N+(p+1)}{N-(p+1)}\right) \tag{A.4}$$

where N is the number of data samples, p is the order, and $\hat{\sigma}_p{}^2$ is the estimated variance at order p. The order p selected is the one for which the FPE value is the minimum. The AIC for an AR process has the following form:

$$\mathrm{AIC}(p) = N \ln\left(\hat{\sigma}_p^2\right) + p \ln(N) \tag{A.5}$$

The criteria presented here may be simply used as guidelines for initial order selection, which are known to work well for true AR signals; but may not work well with real data, depending on how well such data set is modeled by an AR model. Therefore, both FPE and AIC have been adapted in this research for the AR order suggestion.

Figure 3.3 displays an example of FPE and AIC criteria map. The signal used here is the same one shown in Figure 3.2. All rescaled FPE(p) and AIC(p) values at different AR order p are calculated and plotted in Figure A.1. The order searching range is from 1 to 80. The AIC reaches its minimum at p equal to 49. With the FPE, the minimum values are obtained when AR order is 59. Comparing these two orders by looking at their AR spectra, an order of 49 is able to produce a relatively good resolution spectrum while an order of 59 does not improve the resolution by much. Therefore, 49 may be selected as the AR model order for this signal.

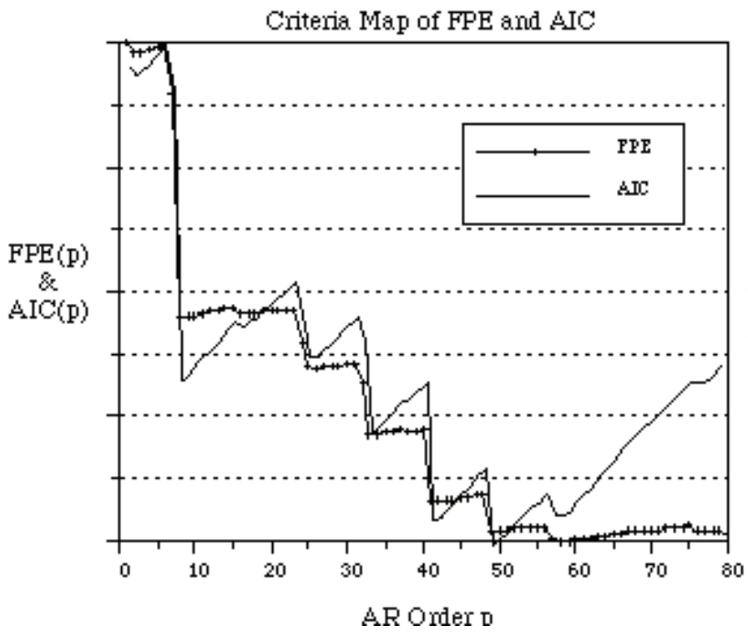

Fig. A.1 Criteria map of FPE and AIC

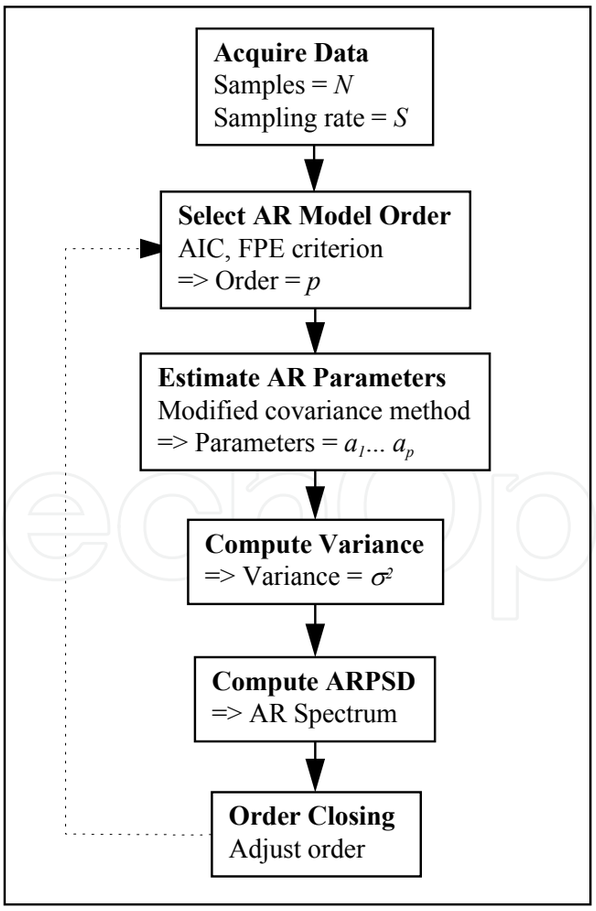

Fig. A.2 AR parameters and PSD estimation flow chart

Fig. A.2 summarizes the flow chart of calculating AR parameters and ARPSD to conclude this section.

5.4 Trending techniques for vibration condition

In order to monitor the condition of a machine throughout its operational life, several vibration trending techniques have been investigated. Vibration trending indices allow the relative machine condition to be plotted with respect to time. From the trending plot most gradual changes relating to the condition of machines can be detected.

Each signal could have more than one trending index associated with it. Furthermore, each trending index, which may be treated as a different aspect of the signal, carries different sensitivities for different machine fault types. In the case of vibration, several trending monitoring techniques have been developed and studied (Mathew, 1989; Dyer & Stewart, 1978; Mathew & Alfredson, 1984; Spoerre, 1993). In this instance, EWMA (Exponential Weighted Moving Average), RMS (Root Mean Square). The mathematical description of each method is given in the following sections.

5.5 ART2 neural network

Adaptive Resonance Theory (ART) is first introduced by Grossberg in 1976 (Grossberg, 1976a). This theory emerged through an analysis of neural networking mechanisms, namely, the hypothetical STM (Short-Term Memory) and the LTM (Long-Term Memory) architectures of the human brain. The theory has been claimed to be capable of self-organizing and self-stabilizing learning in real time in an arbitrarily changing complex input environment (Banquet & Grossberg, 1987; Grossberg, 1976a; Grossberg, 1976b). Over the years, ART has steadily developed as a physical theory to explain cognitive information processing and has been applied to many pattern classification problems (Carpenter et al., 1991).

The architecture designed by the ART algorithm performs pattern clustering and is trained without supervision. Analyses showed this type of top-down feedback learning scheme could significantly overcome the problem of unstable learning, such as local minimum problem in the back propagation algorithm (Grossberg, 1987a).

5.6 Basic concept of the adaptive resonance theory

The basic ART architecture includes two subsystems, an attentional subsystem and an orienting subsystem. When learning or classification occurs within the ART architecture these two functionally complementary subsystems are activated to process familiar and unfamiliar patterns. Fig. A.3 illustrates the anatomy of the ART attentional-orienting system. At first, familiar patterns are processed within the attentional subsystem, which is built up from a competitive learning network. The second subsystem, the orienting subsystem, resets the attentional subsystem when a unfamiliar pattern occurs. Interactions between these two subsystems help to express whether a novel pattern is familiar and well represented by an existing category code, or unfamiliar and in need of a new category code.

In the attentional subsystem two successive stages, the feature representation field (F_1) and the category representation field (F_2), encode input patterns into a form of short term memory. Bottom-up and top-down pathways between F_1 and F_2 contain long term memory traces. Those traces are represented as weight vectors B_{ij} and T_{ji} in Fig. A.3 When a new input pattern arrives, it is then transformed into an activating pattern as an STM form in F_1. This STM pattern is then multiplied, or gated, by the pathway's bottom-up LTM traces.

After the LTM gated signal reaches F_2, the signal is quickly transformed by interactions among the nodes in F_2. The resulting pattern is then stored as another STM in F_2. Just like the new pattern gated by the bottom-up adaptive filter, the STM pattern in F_2 is gated by the top-down LTM traces and summed up as an internal pattern which is then called a top-down template, or learned expectation to F_1. As soon as a top-down template is generated, F_1 acts to match the top-down template against the current STM pattern in F_1. If a mismatch occurs in F_1, the orienting subsystem is engaged, thereby leading to deactivate the current STM in F_2. After that, a new active STM pattern in F_2 is produced. This generates a new top-down template pattern through top-down traces again. The search ends when an STM pattern across F_2 reads out a top-down template which matches the current STM in F_1 to the degree of accuracy required by the level of the vigilance parameter. In this case, the bottom-up and top-down LTM traces are adaptively adjusted according to the current internal STM in F_1. Otherwise, a new classification category is then established as a bottom-up code and a new top-down template is learned.

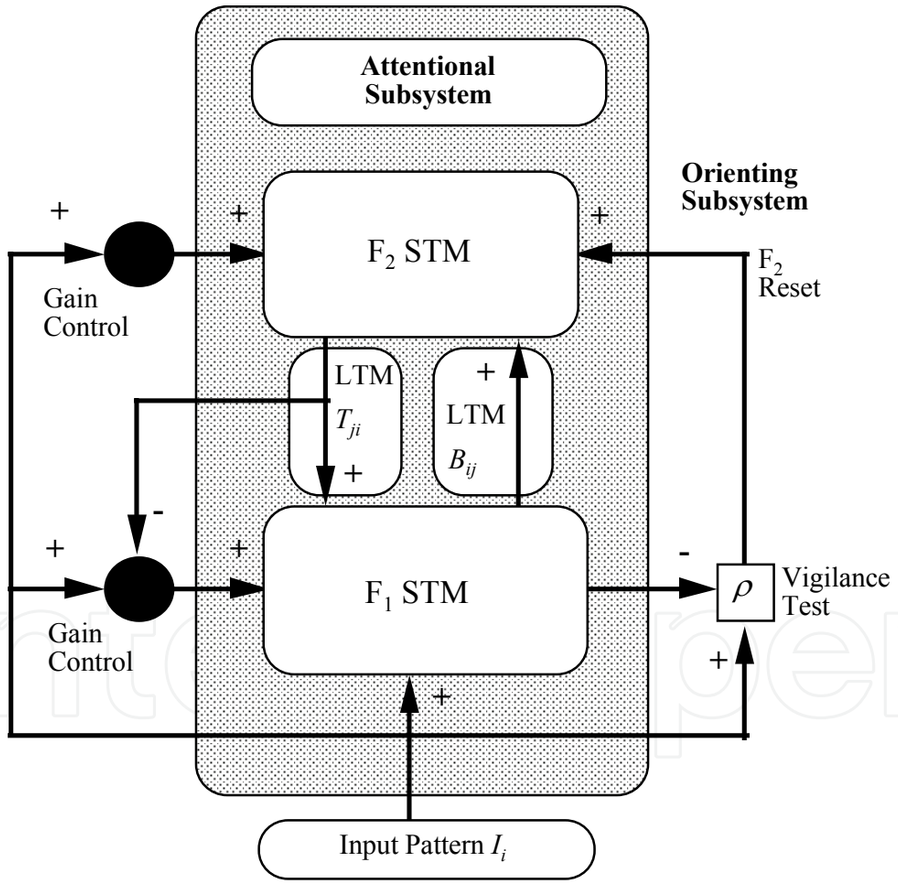

(Adapted from Carpenter and Grossberg, 1987b)

Fig. A.3 typical ART module.

By this fashion, a rapid series of the STM matching and resets may take place. Such an STM matching and reset series controls the system's hypothesis testing and search of the LTM by sequentially engaging the novelty-sensitive orienting subsystem.

5.7 ART2 system dynamics

The mathematical representation of ART2 dynamics is discussed in this section. Fig. A.4 illustrates an ART2 architecture that includes the principal components of ART modules, the attentional subsystem, and the orienting subsystem. In the attentional subsystem, there are three separate fields: an input preprocessing field, F_0, an input representation field, F_1, and a category representation field, F_2. Fig. A.4 also displays the ART2 dynamics by arrows, circles, and filled circles where arrows represent the processing directions and filled circles represent the normalization operations (i.e., Euclidean Normalization).

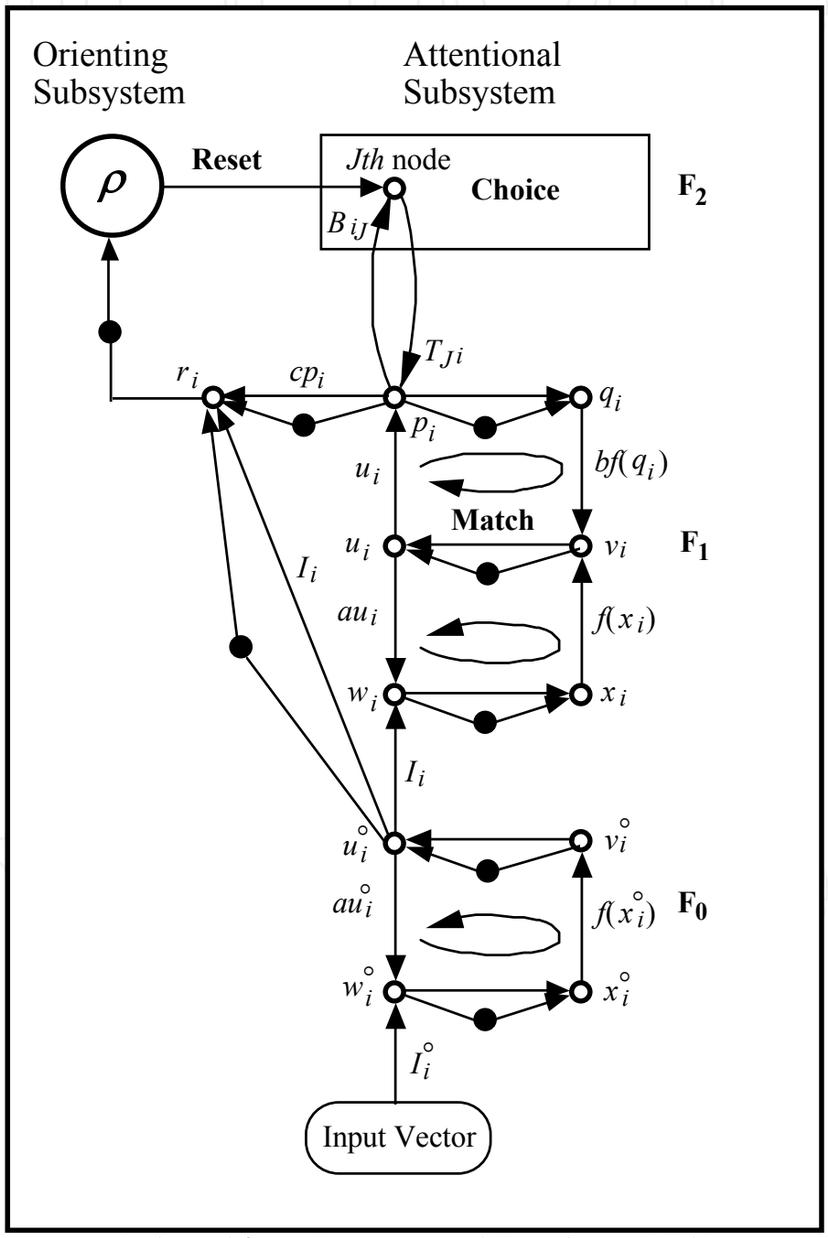

(Adapted from Carpenter and Grossberg, 1987b)

Fig. A.4 ART2 architecture.

6. References

Singh, G. K. & Kazzaz, S. A. S. A. (2003). Induction Machine Drive Condition Monitoring and Diagnostic Research - a Survey, *Electric Power Systems Research,* Vol. 64, pp. 145-158.

Huang, H. -H. (1993). *Transputer-Based Machine Fault Diagnostic, Ph.D. Dissertation,* Department of Industrial Engineering, The University of Iowa, Iowa City, Iowa.

Knapp, G. M. and Wang, H. -P. (1992). Machine Fault Classification: A Neural Network Approach, *International Journal of Production Research*, Vol. 30, No. 4, pp. 811-823.

Knapp, G. M., (1992). *Hierarchical Integrated Maintenance Planning for Automated Manufacturing Systems, Ph.D. Dissertation*, Department of Industrial Engineering, The University of Iowa, Iowa City, Iowa.

Carpenter, G. A. & Grossberg, S. (1987b). ART2: Self-Organization of Stable Category Recognition Codes for Analog Input Patterns, *Applied Optics*, Vol. 26, No. 23, December, pp. 4919-4930.

Carpenter, G. A.; Grossberg, S. & Reynolds, J. H. (1991). ARTMAP: Supervised Real-Time Learning and Classification of Non-stationary Data by a Self-Organizing Neural Network, *Neural Networks*, Vol. 4, pp. 565-588.

Spoerre, J. K. (1993). Machine Performance Monitoring and Fault Classification Using an Exponentially Weighted Moving Average Scheme, Master Thesis, Department of Industrial Engineering, The University of Iowa, Iowa City, IA.

Monk, R. (1972). Vibration Measurement Gives Early Warning of Mechanical Faults, *Process Engineering*, November, pp. 135-137.

Wheeler, P. G. (1968). Bearing Analysis Equipment Keeps Downtime Down, *Plant Engineering*, Vol. 25, pp. 87-89.

Gersch, W. & Liu, T. S. (1976). Time Series Methods for the Synthesis of Random Vibration Systems, *ASME Journal of Applied Mechanical,* Vol. 43, No. 1, pp. 159-165.

Akaike, H. (1969). Power Spectrum Estimation through Autoregression Model Fitting, *Ann. Inst. Stat. Math.*, Vol. 21, pp. 407-419.

Akaike, H. (1974). A New Look at the Statistical Model Identification, *IEEE Transactions on Automation Control*, Vol. AC-19, December, pp. 716-723.

Gersch, W.; Brotherton, T. & Braun, S. (1983). Nearest Neighbor-Time Series Analysis Classification of Faults in Rotating Machinery, *Transactions of the ASME*, Vol. 105, April, pp. 178-184.

Swingler, D. N. (1980). Frequency Errors in MEM processing, *IEEE Transactions on Acoustic, Speech, Signal Processing*, Vol. ASSP-28, April, pp. 257-259.

Kay, S. M. (1988). Modern Spectral Estimation: Theory and Application, Prentice Hall Inc., NJ.

Marple, S. L. Jr. (1987). *Digital Spectral Analysis with Applications*, Prentice Hall Inc., NJ.

Mathew, J. & Alfredson, R. J. (1984). The Condition Monitoring of Rolling Element Bearings Using Vibration Analysis," Journal of Vibration, Acoustics, *Stress, and Reliability in Design,* Vol. 106, July, pp. 447-453.

Mathew, J. (1989). Monitoring the Vibrations of Rotating Machine Elements--An Overview, *ASME*, DE Vol. 18-5, pp. 15-22.

Dyer, D. & Stewart, R. M. (1978). Detection of Rolling Element Bearing Damage by Statistical Vibration Analysis, *Transactions of the ASME Journal of Mechanical Design*, Vol. 100, April, pp. 229-235.

Grossberg, S. (1976a). Adaptive Pattern Classification and Universal I: Parallel Development and Coding of Neural Feature Detectors, *Biological Cybernetics,* Vol. 23, pp. 121-134.

Grossberg, S. (1976b). Adaptive Pattern Classification and Universal II: Feedback Expectation Olfaction and Illusions, *Biological Cybernetics,* Vol. 23, pp. 187-202.

Grossberg, S. (1987a). Competitive Learning: from Interactive Activation to Adaptive Resonance, *Cognitive Science*, Vol. 11, pp. 23-63.

Banquet, J. P. & Grossberg, S. (1987). Probing Cognitive Processes Through the Structure of Event-related Potentials during Learning: an Experimental and Theoretical Analysis, *Applied Optics*, Vol. 26, No. 23, December, pp. 4931-4944.

IntechOpen

IntechOpen

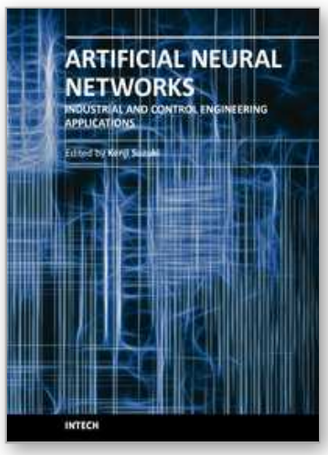

Artificial Neural Networks - Industrial and Control Engineering Applications

Edited by Prof. Kenji Suzuki

ISBN 978-953-307-220-3
Hard cover, 478 pages
Publisher InTech
Published online 04, April, 2011
Published in print edition April, 2011

Artificial neural networks may probably be the single most successful technology in the last two decades which has been widely used in a large variety of applications. The purpose of this book is to provide recent advances of artificial neural networks in industrial and control engineering applications. The book begins with a review of applications of artificial neural networks in textile industries. Particular applications in textile industries follow. Parts continue with applications in materials science and industry such as material identification, and estimation of material property and state, food industry such as meat, electric and power industry such as batteries and power systems, mechanical engineering such as engines and machines, and control and robotic engineering such as system control and identification, fault diagnosis systems, and robot manipulation. Thus, this book will be a fundamental source of recent advances and applications of artificial neural networks in industrial and control engineering areas. The target audience includes professors and students in engineering schools, and researchers and engineers in industries.

How to reference

In order to correctly reference this scholarly work, feel free to copy and paste the following:

Chang-Ching Lin (2011). Intelligent Vibration Signal Diagnostic System Using Artificial Neural Network, Artificial Neural Networks - Industrial and Control Engineering Applications, Prof. Kenji Suzuki (Ed.), ISBN: 978-953-307-220-3, InTech, Available from: http://www.intechopen.com/books/artificial-neural-networks-industrial-and-control-engineering-applications/intelligent-vibration-signal-diagnostic-system-using-artificial-neural-network

INTECH
open science | open minds

InTech Europe
University Campus STeP Ri
Slavka Krautzeka 83/A
51000 Rijeka, Croatia
Phone: +385 (51) 770 447
Fax: +385 (51) 686 166
www.intechopen.com

InTech China
Unit 405, Office Block, Hotel Equatorial Shanghai
No.65, Yan An Road (West), Shanghai, 200040, China
中国上海市延安西路65号上海国际贵都大饭店办公楼405单元
Phone: +86-21-62489820
Fax: +86-21-62489821

© 2011 The Author(s). Licensee IntechOpen. This chapter is distributed under the terms of the Creative Commons Attribution-NonCommercial-ShareAlike-3.0 License, which permits use, distribution and reproduction for non-commercial purposes, provided the original is properly cited and derivative works building on this content are distributed under the same license.

IntechOpen

IntechOpen